Allan Variance Analysis on Error Characters of MEMS Inertial Sensors for an FPGA-based GPS/INS System

Xin Zhang, Yong Li, Peter Mumford, Chris Rizos
School of Surveying and Spatial Information Systems
University of New South Wales, Australia

BIOGRAPHY

Xin Zhang is an undergraduate student of School of Electrical Engineering and Telecommunications, the University of New South Wales (UNSW), Sydney, Australia. He has been involved in the development of a low-cost integrated navigation system using MEMS inertial sensors and GPS on the field-programmable gate array (FPGA) platform.

Dr. Yong Li is a senior research fellow at the Satellite Navigation And Positioning (SNAP) Lab within the School of Surveying & Spatial Information Systems, UNSW. He was involved in the development of a space borne GPS attitude determination receiver, a MEMS inertial sensors/GPS system for a sport application, and a real-time GPS/INS integrated system on a FPGA platform. His current interests include integration of GPS, INS, and pseudolite (Locata), attitude determination, FPGA technology, and its application to navigation, and optimal estimation/filtering theory and applications.

Peter Mumford is a research assistant in the School of Surveying & Spatial Information Systems at UNSW. He is part of the SNAP Lab, specializing in FPGA and embedded software design for GNSS applications. He has an engineering degree in surveying (UNSW) and a science degree in mathematics (Sydney University).

Professor Chris Rizos is a graduate of UNSW, obtaining a Ph.D. in satellite geodesy. He is currently the head of the School of Surveying & Spatial Information Systems at UNSW. Chris has been researching the technology and applications of GPS since 1985 and over a decade ago established the Satellite Navigation and Positioning group at UNSW, today the largest and best known academic GPS and wireless location technology R&D laboratory in Australia. He is the vice-president of the International Association of Geodesy (IAG), and a member of the governing board of the International GNSS Service. He is a Fellow of the IAG and a Fellow of the Australian Institute of Navigation.

ABSTRACT

The combination of GPS/INS provides an ideal navigation system of full capability of continuously outputting position, velocity, and attitude of the host platform. However, the accuracy of INS degrades with time when GPS signals are blocked in environments such as tunnels, dense urban canyons and indoors. To dampen down the error growth, the INS sensor errors should be properly estimated and compensated before the inertial data are involved in the navigation computation. Therefore appropriate modelling of the INS sensor errors is a necessity. Allan Variance (AV) is a simple and efficient method for verifying and modelling these errors by representing the root mean square (RMS) random drift error as a function of averaging time. The AV can be used to determine the characteristics of different random processes. This paper applies the AV to analyse and model different types of random errors residing in the measurements of MEMS inertial sensors. The derived error model will be further applied to a low-cost GPS/MEMS-INS system once the correctness of the model is verified. The paper gives the detail of the AV analysis as well as presents the test results.

INTRODUCTION

Inertial navigation system (INS) has the ability to output its acceleration and angular rate in a high rate. However its accuracy will become degraded along with time due to the combined effects from different types of error sources, such as sensor noises, bias variations, drifts and scale factor instabilities. The errors accumulated with integration of the inertial data in the navigation algorithm will cause the navigation solution drift away from the "true" value quickly. Hence, the knowledge of modelling

and estimating the sensor's errors is a necessity to properly apply the inertial data.

This paper focuses on the stochastic modelling. The transfer function of the system can be estimated from the power spectrum of the output of the system with the input of the white noise. Due to the less restrictive of analysis, the power spectrum density (PSD) and AV method are used for the investigation of INS stochastic process.

Upon the fact that the PSD is the Fourier transform pair of autocorrelation function, the frequency domain approach of using the PSD to estimate transfer functions is straightforward but difficult for non-system analysis [1]. Several variance techniques in the time domain have been proposed [2] [3]. However, they are basically similar and can be primarily distinguished from each other in different signal processing methods applied. For example, the weighting functions and the window functions are incorporated into the analysis algorithms to achieve a particularly desired result by improving the model characterisations [4]. The simplest among them is the AV method.

The AV technique is originally developed in the mid-1960s for studying the frequency stability of precision oscillators [5]. It can help identify the types and magnitudes of the errors residing in the measurements. Because of the close analogies to inertial sensors, this method has been adapted to random-drift characterisation of a variety of devices [6]. The AV is the square of a two-sample deviation which presents sequential average frequency instabilities.

In comparison with other stochastic modelling methods, for example, the autocorrelation method, which needs very long term static data to produce results within an acceptable range [7], the AV method, is straightforward and simple for calculation. It can be applied to testing a board range of sensors including oscillators and inertial sensors.

The paper applies the AV method to characterisation of the MEMS inertial sensors. The procedure is as follows. The characteristic curve is first obtained by applying the AV algorithm to the entire data. The curve is then measured to determine the types and magnitudes of certain random errors possibly residing in the data. Finally, the random errors are identified and modelled.

The paper is organised as follows. The mathematical definition of the PSD and the AV and their relationship are summarised first. Then various error components are sorted out by the slopes on the Allan deviation plot, in which different error mechanisms are separated in different time region. The test results are presented and further works are outlined.

METHODOLOGY

1. Power Spectrum Density

The PSD is the most commonly used in representation of the spectral decomposition of a time series. It is a powerful tool for analysing or characterising data, and stochastic modelling. One way to calculate the PSD from a finite sample path is to take the Fourier transform of the estimate of the autocorrelation function. For a stationary process, the basic relationships between the two-sided PSD and autocorrelation function of a signal are Fourier transform pairs, as shown in the equations below:

$$S(\omega) = \int_{-\infty}^{+\infty} e^{-j\omega\tau} K(\tau) d\tau \quad (1)$$

$$K(\tau) = \frac{1}{2\pi} \int_{-\infty}^{+\infty} e^{j\omega\tau} S(\omega) d\omega \quad (2)$$

where S(ω) is the two-sided PSD, and K(τ) is the autocorrelation function. The autocorrelation function is defined as the cross-correlation of the signal itself with a time difference of τ as below:

$$K(\tau) = \frac{1}{2\pi} \int_{-T+\frac{|\tau|}{2}}^{T-\frac{|\tau|}{2}} x(t+\frac{\tau}{2}) x(t-\frac{\tau}{2}) dt \quad (3)$$

where, $\tau = t_1 - t_2$ is the time difference between two epochs, T is the period, and $|\tau|<2T$.

2. Allan Variance

In the AV method of data analysis, the uncertainty in the data is assumed to be generated by errors of specific characters. The magnitude of each error source covariance is then estimated from the data. The details of the AV and how it is applied to the frequency and time metrology can be found in the literatures e.g. [6] [8]. A brief summary of the AV method is given herein.

Assume N samples of data from an inertial sensor (accelerometer or gyro) with a sample time of τ_0 form groups of data points with the duration $\tau_0, 2\tau_0, \ldots, n\tau_0$, with n< (N-1)/2, and each group is so-called a cluster. Assume the instantaneous output of the sensor is $\Omega(t)$, and its corresponding integration is the angle for example, for the gyros output:

$$\theta(t) = \int^{t} \Omega(t') dt' \quad (4)$$

The lower boundary of the integration is not specified since only the angle differences are employed in the relevant definitions [1]. The angle of the sensor is measured at discrete times given by $t = k\tau_0$, $k=1, 2, 3..., N$. For simplification, the notation is written as $\theta_k = \theta(k\tau_0)$

The average angle rate between times t_k and $t_k + \tau$ is given by

$$\overline{\Omega}_k(\tau) = \frac{1}{\tau}\int_{t_k}^{t_k+\tau} \Omega(t)dt \ , \quad \tau = n\tau_0 \tag{5}$$

The Allan Variance is defined as follows

$$\sigma^2(\tau) = \frac{1}{2} < (\overline{\Omega}_{k+n} - \overline{\Omega}_k)^2 >$$
$$= \frac{1}{2\tau^2} < (\theta_{k+2n} - 2\theta_{k+n} + \theta_k)^2 > \tag{6}$$

where <> denotes an infinite time average. In a practice application, the requirement of infinite time average is never fulfilled [4]. The AV can be then estimated from a finite number of samples by

$$\sigma^2(\tau) \cong \frac{1}{2\tau^2(N-2n)} \sum_{k=1}^{N-2n} (\theta_{k+2n} - 2\theta_{k+n} + \theta_k)^2 \tag{7}$$

The above form of variance is called *overlapped AV*, which can provide better confidence. Note that the definitions above are hold for either the gyros or the accelerometers.

3. Relationship between PSD and Allan Variance

The unique of the relationship that exists between variance (σ^2) and the PSD of the intrinsic random processes is:

$$\sigma^2(\tau) = 4\int_0^{+\infty} S_\Omega(f) \frac{\sin^4(\pi f\tau)}{(\pi f\tau)^2} df \tag{8}$$

where $S_\Omega(f)$ is the two-sided PSD of $\Omega(t)$. In addition, $\Omega(t)$ should be a stationary process, such that its autocorrelation function is independent of time and thus keeps as an even function: $K(\tau) = K(-\tau)$.

Eq. (8) is the key to characterise the random noise PSD from the AV equations. And it interprets that the AV is proportional to the total error power of the gyro rate output when passed though a filter with the transfer function of $\sin^4(x)/(x)^2$. This particular transfer function is the method used to create and operate on the clusters [1]. Eq. (8) also implies that the filter band-pass is determined by the cluster τ. Therefore, by assigned different value of τ, different types of random processes can be confirmed. For identifying and quantifying various random processes, the log-log plot is used for the square root of AV (σ) versus time cluster (τ). An efficient spacing of τ values in a plot of log(σ) vs. log(τ) set $n = 2^p$, where p= 0, 1, 2, 3... [8].

Error Type	PSD (S_Ω)	AV ($\sigma^2(\tau)$)	Comments
Quantisation Noise	$(2\pi f)^2 Q^2 T_s$	$\frac{3Q^2}{\tau^2}$	Q: Quant. noise coefficient
Random Walk	N^2	$\frac{N^2}{\tau}$	N: Random walk coefficient
Bias Instability	$(\frac{B^2}{2\pi})\cdot\frac{1}{f}$ $f \le f_0$	$\frac{2B^2}{\pi}\left[\begin{matrix}\ln 2 - \\ \frac{\sin^3 x}{2x^2}(\sin x + 4x\cos x) \\ +Ci(2x) - Ci(4x)\end{matrix}\right]$	B: Bias instability coefficient. $x : \pi f_0 \tau$ Ci : Cosine integration function [9]
Rate random walk	$\left(\frac{K}{2\pi}\right)^2 \frac{1}{f^2}$	$\frac{K^2\tau}{3}$	K: Rate random walk coefficient
Rate ramp	$\frac{R^2}{(2\pi f)^3}$	$\frac{R^2\tau^2}{2}$	R: Rate ramp coefficient
Correlated Noise	$\frac{(q_c T_c)^2}{1+(2\pi f T_c)^2}$	$\frac{(q_c T_c)^2}{\tau}, \tau \gg T_c$ $\frac{q_c^2}{3}\tau, \tau \ll T_c$	q_c :Noise amplitude T_c :Correlation time
Sinusoidal noise	$\frac{\Omega_0^2}{2}\left[\begin{matrix}\delta(f-f_0) \\ +\delta(f+f_0)\end{matrix}\right]$	$\Omega_0^2\left(\frac{\sin^2 \pi f_0 \tau}{\pi f_0 \tau}\right)^2$	Ω_0 :point Amplitude f_0 :point frequency $\delta(x)$:Delta function

Table 1: Summary of PSD and AV [4]

4. Application of AV to error characterisation

The most attractive feature of AV is its ability to sort out various noise components by the slopes on the root AV (Allan deviation) plot provided the different noise mechanisms are reasonably separated in the frequency and time domain [10].

Errors in typical inertial sensors include white noise, quantisation noise, white rate noise, correlated (Markov) random drift, bias instability (1/*f* or flicker rate), flicker rate ramp (ramp instability), and random rate ramp. In the following analysis, only seven noise terms are considered including, quantisation noise, angle random walk, bias instability, rate random walk, rate ramp, correlated noise

and sinusoidal noise, which are believed to have most impacts on the MEMS inertial sensors. Only the first five errors will be analysed on the testing results, since the correlated noise and sinusoidal noise have minor contributions to the net-sum of the total noises and in most cases they only appear at long time clusters.

These error terms are specified through Eq. (8), and are either known to exist in the sensor or otherwise influence its data. The detailed derivations of these noises are given in [11]. Table 1 clearly shows the relationships between the PSD and the AV. The AV of each error term is obtained through the operation of integration for the corresponding PSD in Eq. (8). Then, the Allan deviation characteristic curve of each error term can be derived by a log-log calculation on the AV equation.

Error Type	log(σ)*vs*.log(τ)	**Curve slope**	**Coefficient value**
Quant. Noise	$\log(\sigma) = -\log(\tau) + \log(\sqrt{3}Q)$	-1	$Q = \sigma(\sqrt{3})$
Random Walk	$\log(\sigma) = -\frac{1}{2}\log(\tau) + \log(N)$	-1/2	$N = \sigma(1)$
Bias Instability	$\log[\sigma\ (f_0)\ ] = \log\left(\sqrt{\frac{2\ln 2}{\pi}} \cdot B\right)$ $\cong \log(0.664B)$	0	$B = \frac{\sigma(f_0)}{0.664}$
Rate random Walk	$\log(\sigma) = \frac{1}{2}\log(\tau) + \log\frac{K}{\sqrt{3}}$	+1/2	$K = \sigma(3)$
Rate ramp	$\log(\sigma) = \log(\tau) + \log\frac{R}{\sqrt{2}}$	+1	$R = \sigma(\sqrt{2})$
Correlated Noise	$\log(\sigma) = -\frac{1}{2}\log(\tau) + \log q_c T_c$ $\log(\sigma) = \frac{1}{2}\log(\tau) + \log\frac{q_c}{\sqrt{3}}$	±1/2	$q_c T_c = \sigma(1)$ $q_c = \sigma(3)$
Sinusoidal Noise	See Fig. 1	+1 -1	See Fig. 1

Table 2: Summary of characteristic curve slope and coefficients' value

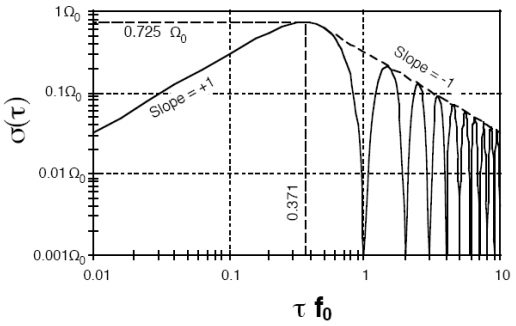

Fig. 1 Allan Deviation plot for sinusoidal noise [6]

From Table 2, it is easy to understand that, in most cases, in different regions of τ appear different error terms. The AV of the total stochastic process can be assumed to be a sum of all the AVs of different error terms, since they are independent on different time regions. The total AV of the system can be then expressed as:

$$\sigma_{tot}^2 = \sigma_{quant}^2 + \sigma_{RW}^2 + \sigma_{Bias}^2 + \sigma_{RRW}^2 \cdots\cdots \qquad (9)$$

A typical AV analysis result is plotted in Fig. 2. However, the shape of curve may be changed enormously due to the unpredictable region length dominated by different error terms.

However, due to the similarity of the curve pattern, some errors can not be recognised by inspection on the characteristic curves, such as white angle, flicker angle have the same curve pattern as quantisation noise, and so as flicker ramp with rate ramp. This is the limitation of AV method. However, these error terms may be sorted out by using the modified AV or pre-whitening methods [4].

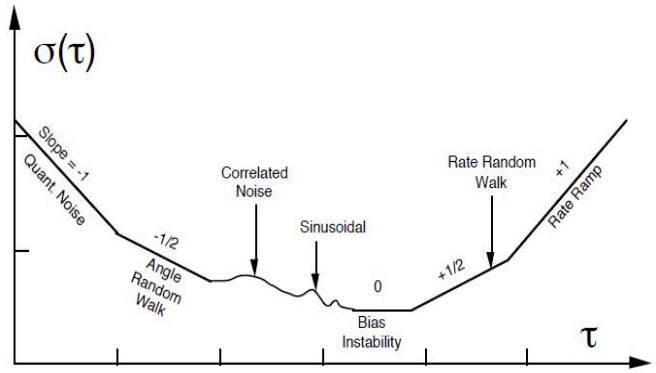

Fig. 2 Typical Allan Deviation plot for a system [6]

TESTING RESULTS

The testing platform is a prototype GPS/INS integrated system, built on an Altera's FPGA development board. The system is developed at the Satellite Navigation and Positioning (SNAP) Lab, within School of Surveying and Spatial Information Systems, University of New South Wales. The real-time time-synchronisation of inertial data with the GPS time has been implemented. The development aims to a low-cost, small-size, and portable navigation system for pedestrians and vehicles [12].

The MEMS inertial sensor used in the system is the MicroStrain's 3DM-GX1, as depicted in Fig. 3. It consists of three angular rate gyros, three orthogonal DC accelerometers, three orthogonal magnetometers, and a 16-bit A/D converter. As stated in the product specification, it has a maximum bias instability of 0.1deg/sec for gyros at fixed temperate angle random walk of 3.5deg/$\sqrt{h}$; and with a bias instability less than 0.01g for accelerometers [13].

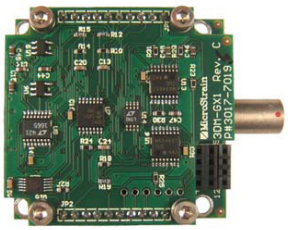

Fig. 3 3DM-GX1

The test was undertaken at a temperature of $20^{o} \pm 3^{o}$ for a period of 2 hours in the SNAP Lab. The tests were repeated in the same testing condition for picking up 5 most stable 2-hour data for the analysis. The accelerometer and gyro data is presented below.

The tri-axial accelerometers, calibrated to provide the acceleration into "g" units measures the reaction force i.e, sum of all forces applied to the sensor that includes the gravity. When the device is horizontally put on a table, the z-axial accelerometer's output of the 3DM-GX1 approximately measures the gravity, which should be eliminated from the measurement before further data processing.

As the analysis method in the previous section, the acceleration and angular rate data are integrated first, such that the instantaneous velocity and angle can be obtained, as indicated in Eq. (5). The infinite-time average method is then applied to get the corresponding averaged acceleration and the angle rate of different time clusters. Finally, a log-log plot is set for the AV and cluster of time, the results for gyros and accelerometers are shown in Figs 4 and 5, respectively.

Fig. 4 obviously shows that the quantisation noise is the dominant term for the short time clusters of the gyro data. For example, in the red curve (x-axial gyro), to extend the line of a slope of -1, one can read a value of $\sigma = 12.475 \text{deg/ h}$ on the extended line at $\tau = \sqrt{3}h$. Therefore, the quantisation coefficient can be determined to be

$$Q_x = 12.475 \text{deg}$$

Similarly, the quantisation coefficients for y and z axes can be determined below,

$$Q_y = 23.636 \text{deg} \quad \text{and} \quad Q_z = 10.505 \text{deg}$$

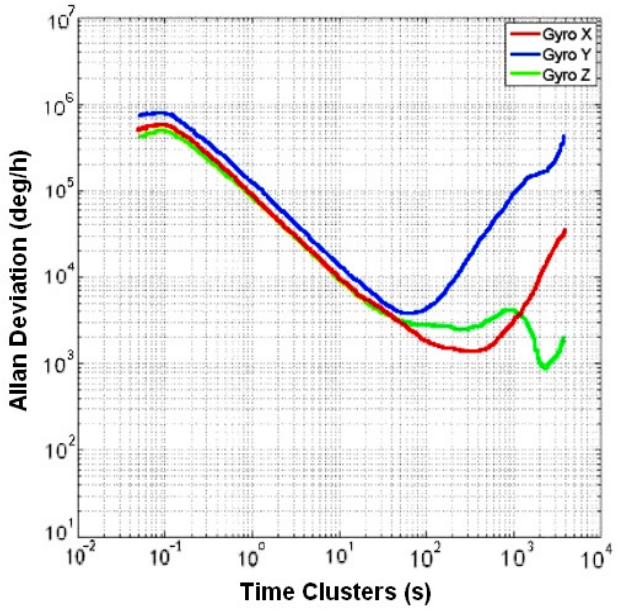

Fig. 4 Allan deviation plot for 3 gyro axes

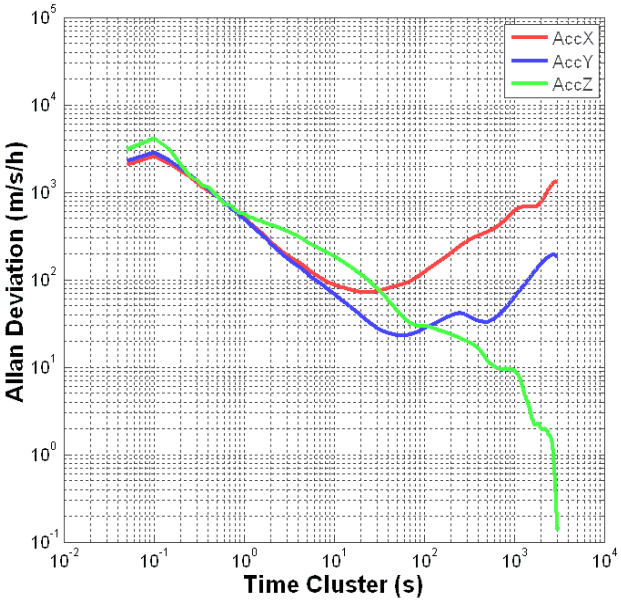

Fig. 5 Allan deviation plot for 3 accelerometer axes

When the time cluster reaches to $\tau = 50s$, the Allan deviations of three axes diverge. The y-axis demonstrates an ascending trend. The y-axial gyro (blue curve) exhibits a slope of +1 due to the effect of rate ramp. A σ-value is $\sigma = 3.348 \times 10^{5} \text{deg/ h}$ on the extended line of the +1 slop at $\tau = \sqrt{2}h$. Hence, the rate ramp coefficient is $R_y = 3.348 \times 10^{5} \text{deg/ h}^2$.

However the x-axial gyro shows a flat region in the time range of 150s-500s, which represents the parameter of the bias instability. One can read the flat line's corresponding σ-value of 1373.152deg/h from the red curve in Fig. 4. Then the reading is divided by a factor of 0.664 to have the instability coefficient of $B_X = 2.068\times10^3 \text{deg/ h}$. The rate ramp coefficient is associated with the ascending line of a slope of +1 on the red curve. Similarly the rate ramp can be read as $R_x = 3.348\times10^5 \text{deg/ h}^2$.

The z-axial gyro is stable in the time range of 50s-500s and the bias instability coefficient can be determined as $B_Z = 2.429\times10^3 \text{deg/ h}$. The curve of z-axial gyro reads like a correlated noise and/or sinusoidal noise when the time cluster $\tau > 500$s.

Overall, the error characters of gyros are summarised in Table 3.

Gyros	x-axis	y- axis	z-axis
Quantisation noise (deg)	$Q_x = 12.475$	$Q_y = 23.636$	$Q_z = 10.505$
Bias instability (deg/h)	$B_x = 2.068\times10^3$	N/A	$B_z = 2.429\times10^3$
Rate ramp (deg/h^2)	$R_x = 2.282\times10^5$	$R_y = 3.348\times10^5$	N/A

Table 3: Identified error coefficients for gyros

Similarly, the different errors of the accelerometers can be characterised through analysing the curves in Fig 5. The Table 4 lists all the identified error coefficients for the accelerometers.

Accelerometers	x axis	y axis	z axis
Quantisation noise (m/s)	$Q_x = 8.5\times10^{-2}$	$Q_y = 8.5\times10^{-2}$	$Q_z = 8.5\times10^{-2}$
Random walk ($\text{m/s}/\sqrt{\text{h}}$)	N/A	N/A	$N_z = 18.2$
Rate random walk ($\text{m/s/h}^{\frac{3}{2}}$)	$K_x = 1.7\times10^3$	$K_y = 298$	N/A

Table 4: Identified error coefficients for accelerometers

From Table 4, one can find that the quantisation noise is dominant at short time clusters for the accelerometers, similar to the gyros. At long time clusters, the rate random walk noise is dominant. The curve of z-axial accelerometer varies at long time clusters and differs from test to test. The phenomenon is possibly caused by the gravity that constantly biases the z-axial accelerometer.

To verify the accuracy of the AV estimation, Table 5 lists all the quantisation noises of gyros from five tests. From the table one can find that the error of the AV estimation can be controlled to a level of smaller than 11%.

Test No.	Gyro X (deg)	Gyro Y (deg)	Gyro Z (deg)
1	12.48	23.64	10.51
2	13.46	21.86	10.67
3	12.54	24.72	11.46
4	12.31	22.39	10.41
5	13.85	26.95	13.33
Average	12.9278	23.9120	11.27
STD	0.6847	2.0303	1.2210
Error%	5.2961	8.4907	10.8310

Table 5: Gyro tests for quantisation noise

CONCLUDING REMARKS

The Allan Variance is a simple and efficient method for identifying and characterising different stochastic processes and their coefficients. Through some simple operations on the sensors output, a characteristic curve of the Allan deviation can be obtained, which can be further used to determine the types and magnitudes of errors residing in the data.

A series of 2-hour tests have been collected using the 3DM-GX1. The results show that the identified errors parameters are close to the manufacture's claim, which proves correctness of the AV method utilised in this paper. From the testing results the conclusion can be drawn that the dominant noise type is quantisation noise for both gyros and accelerometers for the short time clusters. For the long time clusters, the dominant error for the gyros is the rate ramp but the rate random walk for the accelerometers.

When the main stochastic errors are identified and quantified, an error model can be derived and can be applied further to our GPS/INS integrated system.

REFERENCES

[1] N. EI-Sheimy, "Analysis and Modeling of Inertial Sensors Using AV", *IEEE Transaction on instrumentation and measurement,* vol. 57, No.1, JANUARY 2008.

[2] N. K. Sinha and B. Kuszta, , *Modeling and Identification of Dynamic Systems.* New York: Van Nostrand Reinhold, 1983.

[3] J. S. Bendat, and A. G. Piersol *Measurement and Analysis of Random Data.* New York: John Wiley and Sons, 1966.

[4] IEEE Standard Specification Format Guide and Test Procedure for Single-Axis Laser Gyros, *IEEE Std. 647-2006.*

[5] D. W. Allan, "Statistics of atomic frequency standards," Proceedings of the IEEE, vol. 54, no. 2, pp. 221–230, Feb. 1966.

[6] IEEE Standard Specification Format Guide and Test Procedure for Single-Axis Interferometric Fiber Optic Gyros. *IEEE Std. 952-1997.*

[7] H. Hou, "Modeling inertial sensors errors using AV," M.S. thesis, MMSS Res. Group, Dept. Geomatics Eng., Univ. Calgary, Calgary, AB, Canada, UCGE Rep. 20201, Sep. 2004. [Online].Available: *http://www.ucalgary.ca/engo_webdocs/NES/04.20201.HaiyingHou.pdf*

[8] IEEE Standard Definitions of Physical Quantities for Fundamental Frequency and Time Metrology. *IEEE Std 1139™-1988.*

[9] I. S. Gradshteyn and I. M. Ryzhik, *Table of Integrals, series, and Products.* Academic Press, 1980.

[10] H. Kim, *"*Performance Improvement of GPS/INS Integrated System Using AV Analysis*"*, *GNSS International Symposium*, 2004. *http://www.gmat.unsw.edu.au/gnss2004unsw/KIM,%20Hyunseok%20P187.pdf.*

[11] M. M. Tehrani, "Ring laser gyro data analysis with cluster sampling technique," *Proceedings of SPIE*, vol. 412, 1983.

[12] Y. Li, P. Mumford, and C. Rizos, "Seamless navigation through GPS outages – a low-cost GPS/INS solution", *Inside GNSS*, July/August 2008, 39-45.

[13] Microstrain, Technical Product Overview – 3DM GX1, *www.microstrain.com.*